Supporting Information

Tuning Nanoparticle Structure and Surface Strain for Catalysis Optimization

Sen Zhang[1], *Xu Zhang*[2], *Guangming Jiang*[1], *Huiyuan Zhu*[1], *Shaojun Guo*[1], *Dong Su*[3], *Gang Lu*[2] *and Shouheng Sun*[1,*]

[1] Department of Chemistry, Brown University, Providence, Rhode Island 02912, USA

[2] Department of Physics and Astronomy, California State University Northridge, Northridge, California 91330-8268, USA

[3] Center for Functional Nanomaterials, Brookhaven National Laboratory, Upton, New York 11973, USA

[*]Email: ssun@brown.edu

Table of Contents

1. QM-MM Simulations (Text S1)

Core/shell NPs are modeled by cuboctahedrons with eight (111) facets and six (100) facets. The core/shell structure consists of an *fcc*-Pt shell (with three atomic layers) and a FePt or FeCuPt core. The size of NPs is 8 nm corresponding to 10179 atoms in total. ΔE_{O} relative to the flat Pt (111) surface is determined by placing an O atom at the hollow site on the (111) facet of *fcc*-Pt, following

$$\Delta E_{\mathrm{O}} = (E_{\mathrm{QM/MM}}[\mathrm{NP+O}] - E_{\mathrm{QM/MM}}[\mathrm{NP}]) - (E_{\mathrm{QM}}[\mathrm{Pt(111)+O}] - E_{\mathrm{QM}}[\mathrm{Pt(111)}])$$

where $E_{\mathrm{QM/MM}}[\mathrm{NP+O}]$ and $E_{\mathrm{QM/MM}}[\mathrm{NP}]$ are total energies of NPs with and without O adsorbate, respectively from QM-MM calculations. $E_{\mathrm{QM}}[\mathrm{Pt(111)+O}]$ and $E_{\mathrm{QM}}[\mathrm{Pt(111)}]$ are the total energies of the flat Pt (111) surface with and without the absorbed O atom calculated by DFT.

In QM-MM calculations, as shown in **Fig. 2c**, the entire modeled system is partitioned into two spatial domains: a QM region (red, pink and green spheres) treated by constrained DFT [1-3] and a MM region (blue spheres) by empirical atomistic simulations. The QM region is further divided into an interior QM region and a boundary QM region. The former involves bond breaking, chemical reaction and charge transfer, etc. where topological changes of charge density take place. The latter serves as a buffer region where no such topological change to the charge density occurs. The technical details and validations of the QM-MM method can be found elsewhere[4]. The QM region measures 17Å×17Å×8Å in x, y, and z directions, respectively with 195 atoms, where the innermost 8.4Å×7.3Å×4Å is the interior QM region containing the adsorbed oxygen atom on the *fcc*-hollow site. The MM region consists of the rest of the system where the strain effect due to the core/shell lattice mismatch can be captured. The DFT calculations are carried out using the VASP package[5, 6] with the projector augmented wave pseudopotentials (PAW)[7] and Perdew-Burke-Ernzerhof generalized gradient approximation

(PBE-GGA)[8]. The calculations are performed at Γ point with 400 eV energy cutoff. The embedded atom method (EAM) potentials are used in the MM simulations, which have been rescaled to yield the same lattice constant and bulk modulus as those of DFT[9]. The force convergence criterion for atomic relaxation is 0.03 eV/Å.

2. DFT Calculations (Text S2)

A periodic supercell consisting of 108 atoms is used to determine the atomic structure of FePt and FeCuPt core (**Fig 2d, e** and **Fig. S6**). For *fcc*-FePt, 53 Pt atoms and 55 Fe atoms are randomly arranged in the supercell; For *fct*-FePt, 54 Pt atoms and 54 Fe atoms with an alternating layers are arranged in the supercell; For *fcc*-FeCuPt, there are 52 Pt atoms, 27 Fe atoms and 29 Cu atoms randomly arranged; And there are 54 Pt atoms, 28 Fe atoms and 26 Cu atoms in the *fct*-FeCuPt model, where Pt and Fe (or Cu) atom layers are alternating in the supercell; Fe and Cu atoms are randomly arranged in the Fe (or Cu) atom layers. All atoms are fully relaxed under the constant zero pressure by using the DFT calculations. The DFT geometry optimizations are performed using the VASP package with PAW approach and PBE-GGA under the constant (zero) pressure. An energy cutoff of 280 eV is used for the plane-wave basis set. The Brillouin zone is sampled based on the Monkhorst-Pack scheme with a 3×3×3 *k*-point mesh[10]. Spin-polarized DFT calculations are used for all materials under the investigation.

3. Supporting Tables

Table S1. Crystalline lattice constants of FePt and FeCuPt based on DFT calculations.

Materials	$a_{[100]}/a_{Pt}$	$a_{[010]}/a_{Pt}$	$a_{[001]}/a_{Pt}$
fcc-$Fe_{50}Pt_{50}$	0.961	0.964	0.965
fct- $Fe_{50}Pt_{50}$	0.971	0.971	0.945
fcc-$Fe_{25}Cu_{25}Pt_{50}$	0.967	0.963	0.967
fct- $Fe_{25}Cu_{25}Pt_{50}$	0.986	0.985	0.950

a_{Pt} is the lattice constant of *fcc*-Pt. $a_{[100]}$, $a_{[010]}$, $a_{[001]}$ are the calculated interplanar distances along [100], [010] and [001] directions of each material.

4. Supporting Figures

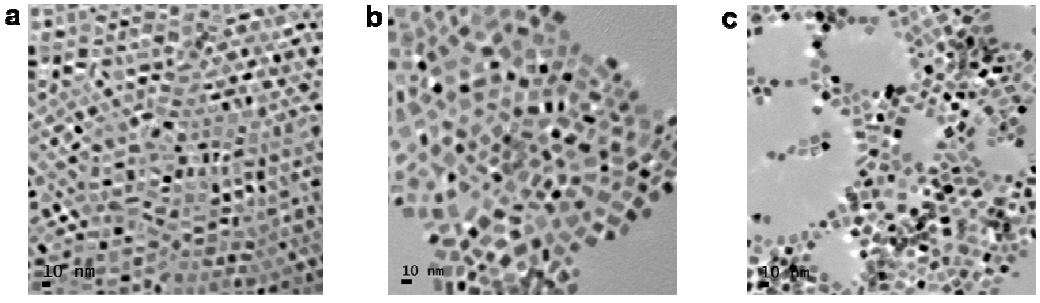

Figure S1. TEM images of the as-synthesized $Fe_{27}Pt_{73}$ (8.7 nm ± 0.6 nm) (**a**), $Fe_{33}Pt_{67}$ (8.5 nm ± 0.4 nm) (**b**), $Fe_{42}Pt_{58}$ (8.3 nm ± 0.4 nm) (**c**) NPs.

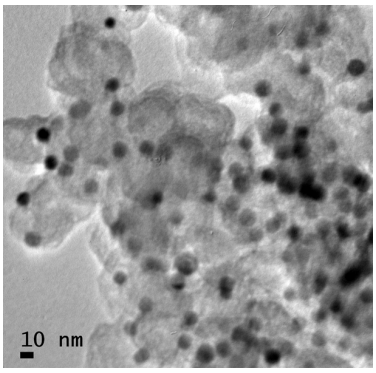

Figure S2. TEM images of the C-$Fe_{51}Pt_{49}$ NPs annealed at 400 ºC.

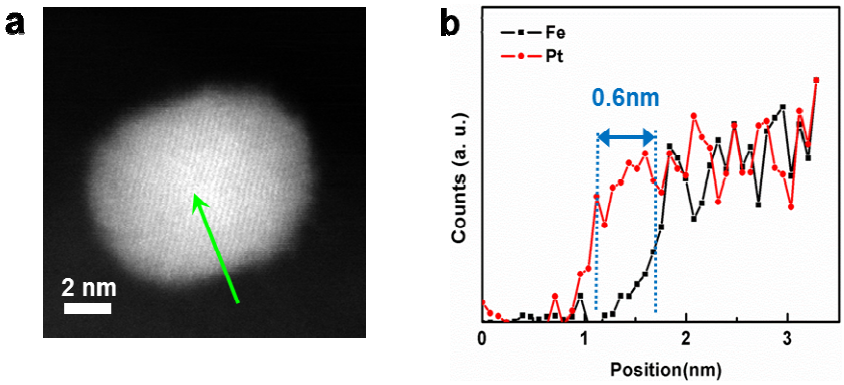

Figure S3. HAADF-STEM image (**a**) and STEM-EELS line scans (**b**) of the electrochemically dealloyed *fcc*-$Fe_{51}Pt_{49}$ NPs, i.e. *fcc*-FePt/Pt NPs. The NPs were annealed at 400 ºC in 95% Ar + 5% H_2 for 1 h. The arrow indicates the line scan position.

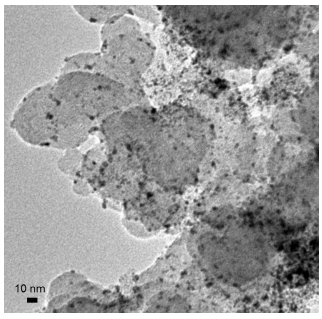

Figure S4. TEM image of the commercial C-Pt catalyst.

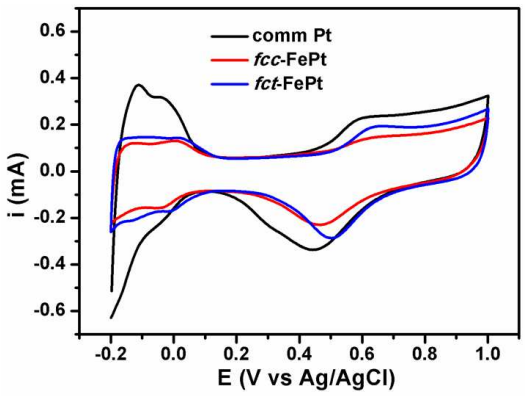

Figure S5. CVs of the commercial Pt, *fcc*-FePt/Pt and *fct*-FePt/Pt NPs. CV's were obtained from N_2-saturated 0.1 M $HClO_4$ with a scan rate of 50 mV/s.

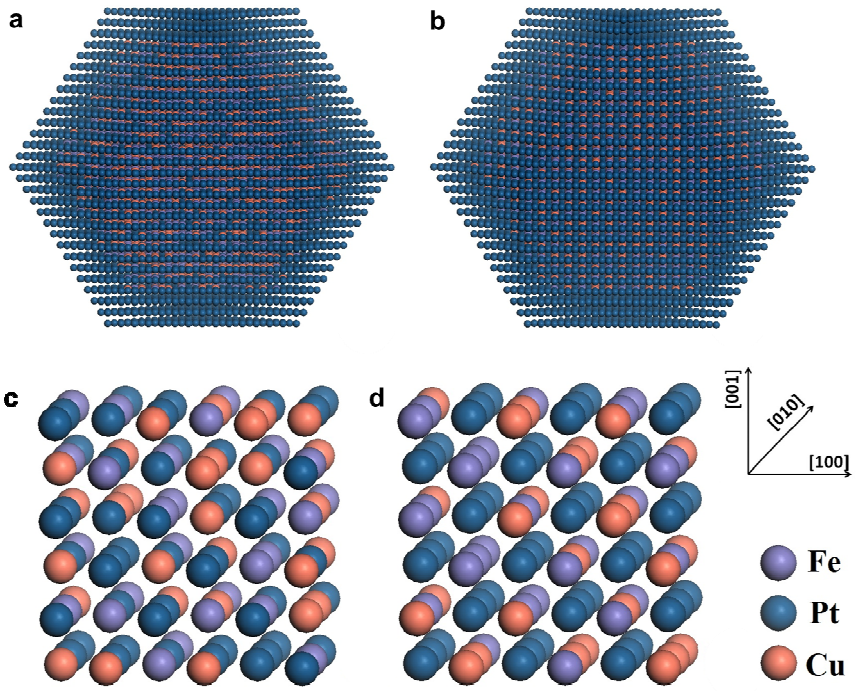

Figure S6. 8 nm cuboctahedral FeCuPt/Pt core/shell NPs models constructed for QM-MM simulations. (**a**) Model for the *fcc*-FeCuPt/Pt core/shell NP with 7667 Pt atoms, 1283 Fe atoms and 1229 Cu atoms. (**b**) Model for the *fct*-FeCuPt/Pt core/shell NP with 7704 Pt atoms 1250 Fe

atoms and 1225 Cu atoms. Two models have a core composition of ~$Fe_{25}Cu_{25}Pt_{50}$ and a three-atom-layer shell of Pt. The blue, purple and orange balls stand for Pt, Fe and Cu atoms, respectively. (**c**, **d**) The periodic supercells of *fcc*-$Fe_{25}Cu_{25}Pt_{50}$ (**c**) and *fct*-$Fe_{25}Cu_{25}Pt_{50}$ (**d**) used to calculate the equilibrium lattice constants.

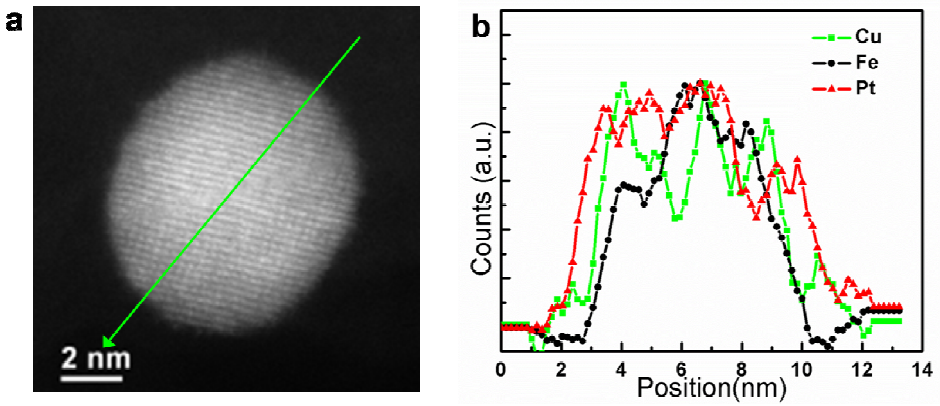

Figure S7. HAADF-STEM image (a) and STEM-EELS line scan (b) crossing an *fcc*-FeCuPt/Pt NP.

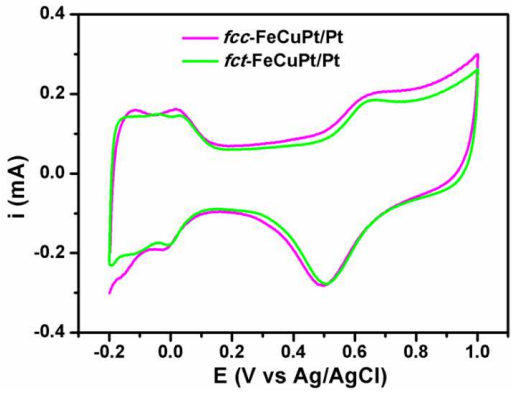

Figure S8. CVs of the *fcc*-FeCuPt/Pt and *fct*-FeCuPt/Pt NPs in N_2-saturated 0.1 M $HClO_4$ with the scan rate of 50 mV/s.

5. Supporting References

1. Zhao, Q. & Parr, R. G. Constrained-search method to determine electronic wave functions from electronic densities. *J. Chem. Phys*. **98**, 543-548 (1993).
2. Zhao, Q., Morrison, R. C. & Parr, R. G. From electron densities to Kohn-Sham kinetic energies, orbital energies, exchange-correlation potentials, and exchange-correlation energies. *Phys. Rev. A* **50**, 2138-2142 (1994).
3. Wu, Q. & Voorhis, T. V. Direct optimization method to study constrained systems within density-functional theory. *Phys. Rev. A* **72**, 024502-024505 (2005).
4. Zhang, X., Lu, G. & Curtin, W. A. Multiscale quantum/atomistic coupling using constrained density functional theory. *Phys. Rev. B* **87**, 054113-054122 (2013).
5. Kresse, G. & Hafner, J. Ab initio molecular dynamics for liquid metals. *Phys. Rev. B* **47**, 558-561 (1993).
6. Kresse, G. & Furthmuller, J. Efficient iterative schemes for ab initio total-energy calculations using a plane-wave basis set. *Phys. Rev. B* **54**, 11169-11186 (1996).
7. Blochl, P. E. Projector augmented-wave method. *Phys. Rev. B* **50**, 17953-17979 (1994).
8. Perdew, J. P., Burke, K. & Ernzerhof, M. Generalized gradient approximation made simple. *Phys. Rev. Lett.* **77**, 3865-3868 (1996).
9. Zhou, X. W., Johnson, R. A. & Wadley, H. N. G. Misfit-energy-increasing dislocations in vapor-deposited CoFe/NiFe multilayers. *Phys. Rev. B* **69**, 144113-144122 (2004).
10. Monkhorst, H. J. & Pack, J. D. Special points for Brillouin-zone integrations. *Phys. Rev. B* **13**, 5188-5192 (1976).